Ultimate strength design of multi-cell rectangular reinforced concrete bridge piers

Autor(en): **Brettle, H.J.**

Objekttyp: **Article**

Zeitschrift: **IABSE publications = Mémoires AIPC = IVBH Abhandlungen**

Band (Jahr): **28 (1968)**

PDF erstellt am: **23.07.2024**

Persistenter Link: https://doi.org/10.5169/seals-22169

Ultimate Strength Design of Multi-Cell Rectangular Reinforced Concrete Bridge Piers

Calcul de la résistance limite des piles de ponts de section rectangulaire, multicellulaire en béton armé

Traglastverfahren für mehrzellige, rechteckige Eisenbeton-Brückenpfeiler

H. J. BRETTLE
Senior Lecturer, School of Civil Engineering, University of New South Wales.

Introduction

During the past thirty years the economical spans of both reinforced concrete and prestressed concrete bridge decks have increased dramatically due to the advent of improved materials, new construction techniques and structural sophistication. This improved technology has permitted the use of thin-wall tee and box section beams which greatly reduces material quantity and has resulted in many extremely graceful deck profiles. In the same period technological advances have not produced similar thin-wall bridge piers.

Publications in structural journals indicate far more interest with structural systems subjected to flexure than with frameworks loaded mainly in compression. This could be due to the simpler theory for solution of flexure problems and to the case of application of large bending moments to full sized flexural members to verify such theory. Although the greatest savings have occurred in deck systems, effort should be made to minimise the cost of the complete bridge including the substructure, consequently a study of bridge pier design has been commenced by the author.

Greater economy will probably result from the use of smaller quantities of material placed at more appropriate positions and sustaining higher average stresses. Ultimate strength analysis should predict the collapse load of such structural members and as the latest codes tend to include lower load factors less material will continue to be required. Such matters as crack widths, deflection, vibration, fatigue, etc., will become more important but it is

probable that the minimum material will result from using the least load factor with ultimate strength design.

Bridge piers are subjected to axial loads and to horizontal forces both along and transverse to a bridge centre line. The lateral forces are minimised by restricting pier end widths and the longitudinal forces greatly decreased by using low friction type bearings. Piers usually traverse the full width of a bridge deck consequently narrow rectangular shapes often result. Large rectangular piers of solid section are usually far too strong for the loads imposed so thin-walled members were considered. A method of analysing rectangular thin-wall reinforced concrete members subjected to compression and biaxial bending was therefore untertaken to determine a satisfactory ultimate strength design procedure.

Since ultimate strength analysis for biaxial bending presents considerable computational difficulties, unsymmetrical reinforced concrete columns are rarely proportined in design practice to carry their ultimate loads. To the author's knowledge no design procedure or method has been published for either the ultimate strength or permissible working stress design of hollow rectangular reinforced concrete members subjected to biaxial bending when tensile stress exists over portion of the cross-section. However, approximate methods [1, 2] and graphs [3, 4] are available for the design of the simplest cases of solid square or rectangular columns containing symmetrically placed reinforcement and subjected to biaxial bending.

BRETTLE and WARNER in a previous paper [12] have produced a general method of analysis of reinforced concrete members of any arbitary cross-section for both ultimate strength and working stress design when subjected to compression and biaxial bending. The method has been developed for use with a digital computer and used to prepare graphs for the ultimate strength design of solid rectangular sections [13].

In this paper the method is adapted for the analysis of hollow rectangular and hollow triple box sections of various width to depth ratios. Design charts have been included for the ultimate strength design of such sections.

Notation

P_0 axial load at failure with zero eccentricity
P_u load at failure having double eccentricities
b overall width of a rectangular cross-section
b' distance in the x direction between centre lines of steel layers adjacent to the sides of the member
b'' width of hollow rectangular areas within the cross-section
t overall depth of a rectangular cross-section
t' distance in the y direction between centre lines of steel layers adjacent to the top and bottom faces of the member

t'' total depth of hollow rectangular areas within the cross-section

C_{ij} elements of a rectangular array C used to define the shape of the concrete cross-section

x_{cj}/b non-dimensionalised x co-ordinates of centroids of regularly spaced array elements C_{ij}

y_{ci}/t non-dimensionalised y co-ordinate of centroids of regularly spaced array elements C_{ij}

X_{cj} a rectangular array whose elements are the x_{cj} co-ordinates of the elements C_{ij} when the array C has irregular column widths

Y_{ci} a rectangular array whose elements are the y_{ci} co-ordinates of the elements C_{ij} when the array C has irregular row depths

S_{ij} elements of a rectangular array S used to define the position and relative magnitude of the steel reinforcement

x_{sj}/b non-dimensionalised x co-ordinates of centroids of regularly spaced array elements S_{ij}

y_{si}/t non-dimensionalised y co-ordinates of centroids of regularly spaced array elements S_{ij}

X_{sj} a rectangular array whose elements are the x_{sj} co-ordinates of the elements S_{ij} when the array S has irregular column widths

Y_{si} a rectangular array whose elements are the y_{si} co-ordinates of the elements S_{ij} when the array S has irregular row depths

n_{cb} number of columns in arrays C, X_{cj} and Y_{ci}

n_{ct} number of rows in arrays C, X_{cj} and Y_{ci}

n_c total number of elements that replace the total concrete area

A_c total concrete area

ΔA_c area of a concrete element $= A_c/n_c$

ΔA_{cij} concrete area ΔA_c at the (i,j)th location of array C

n_{sb} number of columns in arrays S, X_{sj} and Y_{si}

n_{st} number of rows in arrays S, X_{sj} and Y_{si}

n_s total number of elements that replace the total steel area

A_s total steel area

ΔA_s area of steel element $= A_s/n_s$

ΔA_{sij} steel area ΔA_s at the (i,j)th location of array S

p steel proportion $= A_s/A_c$

e_x eccentricity of loading in the x direction measured from the plastic centroid of the cross-section

e_y eccentricity of loading in the y direction measured from the plastic centroid of the cross-section

e_r resultant eccentricity $= \sqrt{e_x^2 + e_y^2}$

e'_x eccentricity of loading in the x direction measured from the point of maximum compressive strain used as the origin shown in Figs. 2 and 3

e'_y eccentricity of loading in the y direction measured from the point of maximum compressive strain used as the origin shown in Figs. 2 and 3

z distance to any fibre measured from the origin in a direction perpendicular to the neutral axis

z_m maximum value of z

z_n perpendicular distance from neutral axis to the origin

θ angle defining the inclination of the neutral axis with respect to the x axis

ψ angle defining the direction to the point of application of the eccentric load P_u with respect to the x axis

ϵ_c concrete strain

ϵ_{cij} concrete strain at centroid of the (i,j)th elemental area ΔA_{cij}

ϵ'_c maximum concrete compressive strain at failure of an axially loaded concrete section

ϵ_{cu} maximum concrete compressive strain at failure of a thin flanged hollow rectangular section subjected to uniaxial bending about a principal axis and when the neutral axis is within the section

$\epsilon_{cu\theta}$ maximum concrete compressive strain at failure of a thin webbed rectangular section when subjected to biaxial bending about any axis

ϵ_u maximum concrete compressive strain in a section at failure

f_c concrete stress

f_{cij} concrete stress at centroid of the (i,j)th element ΔA_{cij}

f'_c concrete control cylinder strength

k_1 ratio of concrete strength in a compression member to its control cylinder strength

k_2 dimensionless parameter reflecting the effect of inclination of neutral axis angle θ, on the ultimate strain.

ϵ_s steel strain

ϵ_{sij} steel strain at centroid of the (i,j)th elemental area ΔA_{sij}

ϵ_{sy} steel yield strain

f_s steel stress

f_{sy} steel yield stress

q reinforcement ratio $= \dfrac{p f_{sy}}{k_1 f'_c}$

q' $q \dfrac{n_c}{n_s}$

q'' $q \dfrac{A_c}{n_s}$

R_c non-dimensionalised concrete stress $= \dfrac{f_c}{k_1 f'_c}$

R_{cij} value of R_c at centroid of the (i,j)th elemental area ΔA_{cij}

R_s non-dimensionalised steel stress $= f_s/f_{sy}$

R_{sij} value of R_s at centroid of the (i,j)th elemental area ΔA_{sij}

R_{s0} value of R_s for all elements ΔA_s when axial load P_0 is applied

S_c normalised concrete strain $= \epsilon_c/\epsilon'_c$

S_s normalised steel strain $= \epsilon_s/\epsilon_{sy}$

Material Properties in Thin-Wall Members

To the author's knowledge no test results are yet available on the physical characteristics of hollow rectangular concrete sections. This may be due to the difficulty in application of the large longitudinal forces required to cause failure of reasonably sized members. It is, therefore, necessary to examine test results of members whose dimensions and shape are similar or equivalent to portions of hollow rectangular bridge piers to permit a reasonable approximation of the required properties.

A multi-cell rectangular cross-section consists of a set of thin walls joined together at their edges. Some experimental work has been reported on plain concrete and lightly reinforced walls without end constraint, which should provide conservative data for the prediction of the strength characteristics of continuously reinforced intersecting walls in a bridge pier. In addition various codes provide instruction for the design of thin reinforced concrete walls.

Ultimate strength tests carried out at the British Building Research Station [5] have shown that uniformly distributed axial force applied to unreinforced concrete walls of height/thickness ratio less than 30, caused material collapse rather than buckling failure when the average axial compressive stress reached 85% of the cylinder strength f'_c. When small quantities of both horizontal and vertical reinforcement were placed adjacent to both wall faces collapse occurred when the average crushing strength equalled f'_c and the steel yielded. Whereas two layers of steel appreciably increased the apparent concrete strength, a single steel layer only increased the wall carrying capacity by the steel area times its yield stress.

The ACI building code [6] includes recommendations for both working stress and ultimate strength design of reinforced walls. It suggests a minimum wall thickness of $^1/_{25}$ of the unsupported height or width which ever is the least. For walls of 10″ thickness or more, two layers of steel are required, one placed adjacent to each wall face where the minimum proportion of vertical and horizontal reinforcement is 0.0015 and 0.0025 respectively.

The Australian concrete building code [7] only permits working stress design and indicates a minimum proportion of vertical and horizontal steel of 0.002. In walls of 8″ or greater thickness two layers of steel, one layer placed adjacent to each face is required. When the distance between adjacent walls is less than the height then the length/thickness ratio becomes the slenderness ratio. If the slenderness ratio exceeds 15 the strength reduction factor for tied columns should be used.

Until such time as test results of hollow rectangular sections are available, the following design restrictions should be adopted when proportioning bridge pier walls. The minimum wall slenderness ratio to be maintained at 20. A minimum steel proportion of 0.002 to be used for both the vertical and hori-

zontal reinforcement. The steel to be placed in two layers, one adjacent to each wall face. It should be noted, however, that this paper does not deal in any way with the instability problem and the above comments are only suggested for the guidance of designers.

The above restrictions apply to walls subjected to reasonably concentric loads occurring in buildings hence the strain distribution is essentially uniform across the walls. A bridge pier can of course be subjected to large bending moments and small axial force consequently the thin-wall flanges can be subjected to linearly varying strain distribution. RÜSCH [9] experimentally examined the strain distribution across beams of various cross sections subjected to pure bending and showed that the extreme fibre strain at failure was about 0.0043 for a solid triangular section and 0.0022 for a thin top flange tee section, when loads were applied for short duration to medium strength concrete. The difference in the value of limiting strain at the extreme fibre depends on the support given to it by adjacent fibres. In thin flanged tee beam specimens the strain distribution across the flange in pure bending is essentially uniform so all fibres tend to fail at the same lower value of limiting strain of 0.0022. When failure occurs in a thin flange hollow rectangular section such that maximum strain occurs along a face of the section, the limiting value of strain ϵ_{cu} will be assumed in this study to equal 0.0022 as in the case of a thin flanged tee beam. The limiting value of strain usually adopted for solid rectangular sections is 0.0035 which increases to 0.0043 in solid triangular sections when maximum strain occurs at a corner. Collapse can also occur at the corner of a hollow rectangular section at a strain value somewhere between these two limits and the lower value was considered as the appropriate conservative value.

Concrete stress-strain curves obtained from axially loaded cylinders vary non-linearly from zero stress up to some maximum strength f'_c at a strain ϵ'_c. The stress then decreases with increasing strain. Final failure depends on the proporties of the test machine and the duration of the test. Whereas the final failure strain varies within wide limits, the value of ϵ'_c remains reasonably constant at about 0.002 [8] for a large range of f'_c values.

The actual stress-strain curve of a concrete specimen is shown in Fig. 1. In an axially loaded specimen the strain ϵ'_c at which f'_c first occurs is assumed to be 0.002. For eccentric loading of a hollow rectangular section, the limiting value of extreme fibre strain can vary from $\epsilon_{cu} = 0.0022$ for a thin-flange beam to $k_2 \epsilon_{cu} = 0.0035$ at the corner of a thin-web rectangular section where k_2 is a dimensionless parameter related to the relative orientation of the rectangular compression zone at failure. The value of k_2 is therefore taken as 1.6 in this paper. The actual concrete stress strain curve can be idealised as shown in Fig. 1 where the stress increases linearly from zero to a maximum value $k_1 f'_c$ at a strain of ϵ'_c where the dimensionless parameter k_1 is the ratio of the concrete stress in a thin-wall rectangular compression member to its control

cylinder strength f'_c. The strain can then increase to any value between ϵ'_c and $k_2 \epsilon_{cu}$ while the stress remains constant at $k_1 f'_c$.

The author has previously compared the effect on the computed ultimate strength of using three quite different stress-strain relations [12]. The ultimate capacity of solid square sections having symmetrically placed reinforcement were computed for rectangular, trapezoidal and curvilinear concrete stress-strain curves and showed a maximum variation of only 10% in the theoretical failure loads for the three cases. Since the trapezoidal or elasto-plastic shape

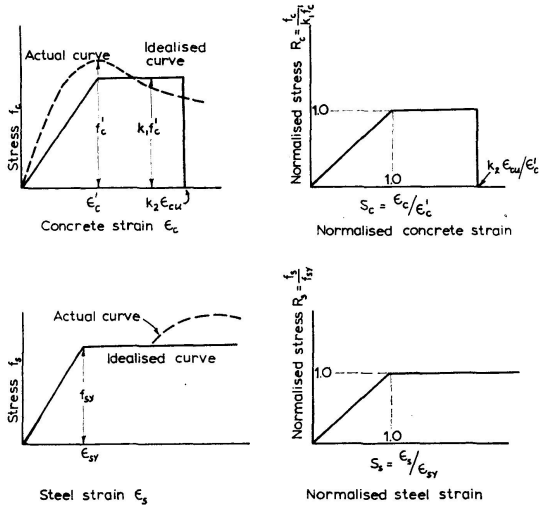

Fig. 1. Stress-strain relations of concrete and steel.

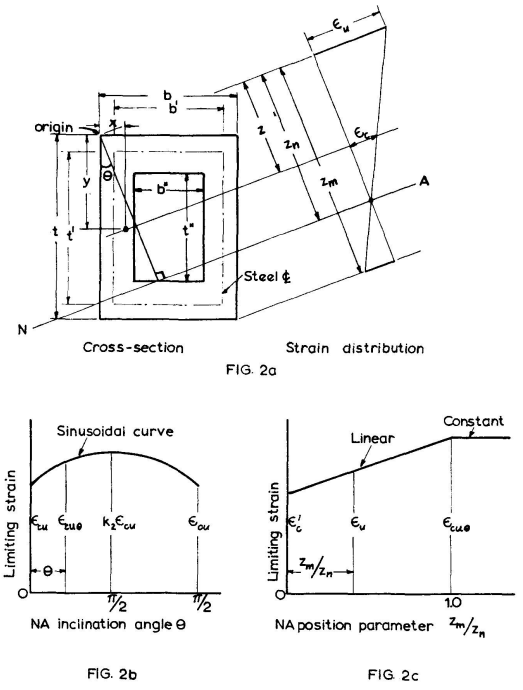

Fig. 2. Limiting values of extreme fibre strain related to inclination and position of the neutral axis.

gave results intermediate between the results of both the rectangular and the curvilinear or polynomial curves, it was adopted in the present investigation.

It was convenient to use non-dimensionalised stress-strain relations in the computational work, and the terms R_c and S_c were introduced where $R_c = f_c/k_1 f'_c$ and $S_c = \epsilon_c/\epsilon'_c$. The idealised elasto-plastic, non-dimensionalised, normalised stress-strain relation adopted for concrete is shown in Fig. 1. Similarly an idealised elasto-plastic stress-strain curve was adopted for steel with no imposed limiting value of strain. Again the ordinates were non-dimensionalised by introducing R_s and S_s where $R_s = f_s/f_{sy}$ and $S_s = \epsilon_s/\epsilon_{sy}$. The non-dimensionalised normalised stress-strain curve adopted for steel is also shown in Fig. 1.

Method of Solution by Partitioning Cross-Section

A section subjected to compression and biaxial bending fails at particular combinations of axial force P_u and bending moments about two axes. When axes through the plastic centroid are used and e_y and e_x are the eccentricities of the point of application of P_u measured perpendicular to these axes as shown in Fig. 3a, the moments at failure become $P_u e_y$ and $P_u e_x$. Solution of the problem requires the summation of stresses multiplied by the areas over which they act in the direction of the column axis and summation of the first moment of the resulting elemental forces about both axes.

Provided a member cross-section is either solid circular or hollow circular and the steel assumed uniformly distributed as a thin annulus around the section, algebraic equations can be formulated and exact solutions obtained [10, 11] even when the stress distribution is non-linear at failure. When a non-linear stress distribution is imposed on an irregular concrete cross-section having randomly placed steel, the formulation of algebraic equations becomes difficult and their solution rather tedious.

To overcome the analytical difficulties a member can be partitioned or subdivided into small discrete elemental areas. Assuming stress-strain relations for both the concrete and steel the strains and hence stresses at the centroids of the small elements can be found. The process of summing the forces acting on the small elements is ideally suited for digital computer solution which replaces the complicated integration of discontinuous functions over irregular areas. Obviously no great difficulty is imposed on computer summation when highly irregular sections are subjected to stress-strain curves of any conceivable shape.

The cross-section of a hollow rectangular multi-cell concrete member can be most simply subdivided by a rectangular grid. If the number of columns in a grid is n_{cb} and the number of rows is n_{ct} then the total number of discrete elements n_c in the hollow section shown in Fig. 3b becomes $n_c = 2\,(n_{cb} + 2\,n_{ct} - 4)$. Provided the grid lines are regularly spaced in both directions, an elemental area $\Delta A_c = \dfrac{A_c}{2\,(n_{cb} + 2\,n_{ct} - 4)}$. Denoting the elemental area at the (i, j)th position of the grid by ΔA_{cij} then the x and y co-ordinates of the centroid of the ele-

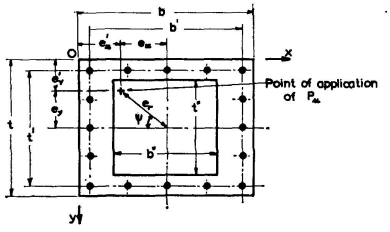

Fig. 3a. Cross-section.

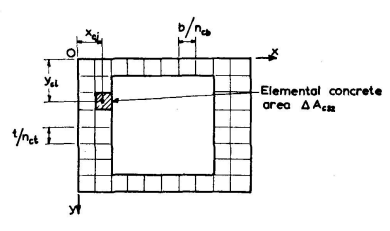

Fig. 3b. Partitioned concrete.

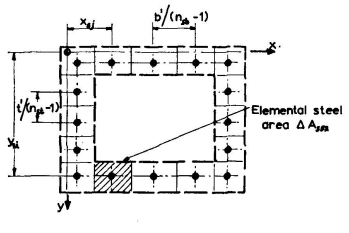

Fig. 3c. Partioned steel.

Fig. 3. Concrete and steel partitioned areas.

ment ΔA_{c32} shown in Fig. 3b measured from the origin at the top left hand corner of the section where the compressive strain is a maximum are, $x_{cj} = 1\frac{1}{2}\, b/n_{cb}$ and $y_{ci} = 2\frac{1}{2}\, t/n_{ct}$ respectively.

Similarly another rectangular grid can be used to subdivide the steel area into elemental areas ΔA_s where the element at the (i,j)th location is denoted by ΔA_{sij}. If the bars are distributed around a section as shown in Fig. 3a, such that equal quantities of steel are placed on opposite faces, then n_{sb} can represent either the number of bars or the number of steel elements assumed to represent the steel placed adjacent the top and bottom faces of a section and n_{st} can represent the steel elements adjacent the side faces. The total number of steel elements n_s in the section shown in Fig. 3c equals $2\,(n_{sb} + n_{st} - 2)$. Provided the grid lines defining the positions of the centroids of the steel elements are regularly spaced in both directions, the elemental steel area $\Delta A_s = \dfrac{A_s}{2\,(n_{sb} + n_{st} - 2)}$. The x and y co-ordinates to the centroids of the steel element ΔA_{s52} shown in Fig. 3c measured from the origin at the top left corner of the section are

$$x_{sj} = \frac{b - b'}{2} + \frac{b}{n_{sb} - 1}$$

and $y_{si} = \dfrac{t - t'}{2} + \dfrac{4\,t'}{n_{st} - 1}$ respectively. The steel elemental areas ΔA_s can be expressed in terms of steel proportion p and concrete elemental areas as:

$$\Delta A_s = \frac{A_s}{n_s} = p\,\Delta A_c \frac{n_c}{n_s}.$$

These simple relations can be used to generate the co-ordinates of the elements and the computer *DO* statement used for their incrementation.

Although a highly irregular area and its properties can be approximated by an extremely fine grid, it is preferable to use an irregularly spaced grid of coarser dimensions to exactly define the cross-section properties. An array of numbers with values equal to the relative areas of the elements can be more easily read into the computer than by *DO* statement incrementation. An array called C whose (i, j)th element is denoted by C_{ij} is included in Fig. 4 for a hollow multi-cell cross-section. In addition an array X_{cj} whose elements are the x_{cj} dimensions to the centroids of the C_{ij} elemental areas together with an array Y_{ci} whose elements fix the y_{ci} distances to the centroids of C_{ij} measured from the origin are also given in Fig. 4.

Similarly random distribution of elemental steel areas can be more easily represented by an array S whose (i,j)th element is denoted by S_{ij} and represents the relative area of the steel elements at that location. An array X_{sj} has elements which indicate the x_{sj} dimensions to the centroids of the steel elements ΔA_{sij} and an array Y_{si} gives values of y_{si} distances measured from the same origin. Since steel bars tend to be uniformly distributed around the walls in bridge pier designs, the co-ordinates of the elements are then simply incre-

mented by the *DO* statement. A typical array S for the relative areas of a regularly spaced steel grid is given in Fig. 5 together with an array C for a regularly spaced concrete grid.

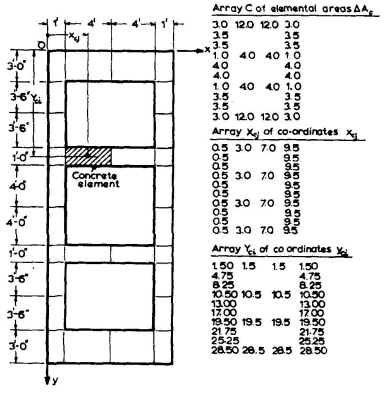

Fig. 4. Concrete section dimension arrays.

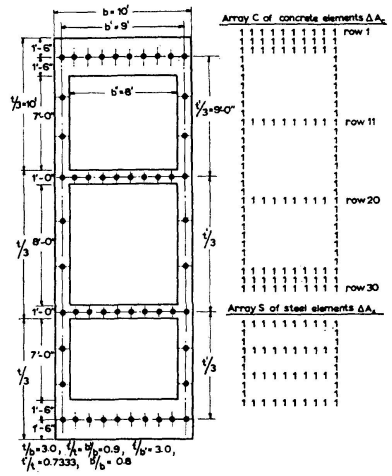

Fig. 5. Dimensions and arrays representing cross-section area.

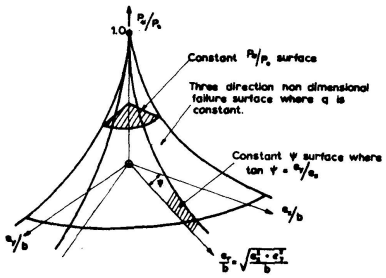

Fig. 6. Graphical representation of column failure surface.

To determine the effect of grid fineness on the ultimate capacity of solid rectangular columns in a previous paper [12], the number of concrete elements was varied from 100 to 900 with a resultant change of only 2% in the ultimate strength. In the present study a 10×10 grid size was therefore selected for the hollow rectangular sections and a 10×30 grid adopted for the triple box sections, to simplify the computation of data for multi-cell pier design charts.

Although a steel proportion of 0.08 can be used in the design of solid rectangular columns, the trend is to use fewer numbers of large diameter bars or few bundles of bars; to minimise the quantity of ligatures required to adequately support all bars in two perpendicular lateral directions. Several authors [3, 4] have published design charts for rectangular sections having 4 to 16 bars, indicating this to be an important variable affecting ultimate strength. However in bridge pier design many bars in double layers are used and a 10×10 grid was adopted to dimension the equivalent steel elemental areas in the generation of data for this paper.

It is apparent from Figs. 3 and 5 that three separate dimensions are required to fix a pier section in the x direction and three dimensions in the y direction i.e. b, b' and b'' denote the overall width, the distance between centres of steel layers adjacent the wall side faces and the inner hole width dimension and t, t' and t'' the overall depth, the distance between centres of steel layers adjacent the top and bottom faces and the total of the inner hole depth dimensions. Assuming the mean position of the steel layers in the walls is located at the mid-wall position and the wall thickness is neglegibly small compared to the pier overall dimensions, then b' can replace b and b'' and t' can replace

t and t''. This means that four variables become redundant and fewer charts need be prepared for the ultimate strength design of piers. This approximation shifts the origin shown in Figs. 2 and 3 to the mid-wall position and column collapse occurs when the concrete strain reaches some upper limiting value at the mid-wall position and not at the extreme fibre position as previously assumed. Although wall thickness has a marked effect on the ultimate force P_u it is shown in a later section that the assumption of thin-walls has little effect of the axial force ratio P_u/P_0 consequently this approximation was made in this paper. It should be noted this same approximation was made in a previous paper [10] relating to hollow circular sections and when the ratio of wall thickness to the mean wall diameter was varied from 0 to 0.2, the ultimate strength capacity changed by only 7%.

Ultimate Strength Analysis

Strain distribution

Several simplifying assumptions relating to reinforced concrete structures were adopted to assist in developing the analysis. The strain distributions remains linear up to failure, perfect bond exists between concrete and steel so that the concrete strain ϵ_c equals the steel strain ϵ_s at a particular fibre and concrete cannot sustain tensile stress.

The location of the neutral axis and its direction are fixed by the loading and section properties. Its position can be defined by some distance z_n measured perpendicular from the neutral axis direction to the position of maximum compressive strain shown as the origin in Fig. 2a and its inclination from the $0x$ axis, denoted by the angle θ. When x and y are the usual co-ordinates measured from the same origin then the distance z to an element is,

$$z = x \sin\theta + y \cos\theta. \tag{1}$$

Similarly when b is the overall width and t the overall depth of a section, the maximum value of z denoted by z_m, measured to the extreme fibre at the lower right hand corner on the section shown in Fig. 2a is,

$$z_m = b \sin\theta + t \cos\theta. \tag{2}$$

If the neutral axis is within a hollow section and parallel to a side failure is imminent in the thin rectangular compression flange when the extreme fibre strain reaches ϵ_{cu}. When the neutral axis is inclined at 45° to either wall face the resulting hollow triangular section is assumed equivalent to a thin webbed rectangular member and the extreme fibre strain increases to $k_2 \epsilon_{cu}$ at failure. Since the value of extreme fibre strain is affected by the orientation of the thin rectangular section at failure, it can be related to the angle of inclination θ of the neutral axis. Denoting the strain by ϵ_{cu} and

adopting the simple sinusoidal relation given in Fig. 2b, the value of $\epsilon_{cu\theta}$ can be obtained from the normalised equation as,

$$\frac{\epsilon_{cu\theta}}{\epsilon'_c} = \frac{\epsilon_{cu}}{\epsilon'_c}[1+(k_2-1)\sin 2\theta]. \tag{3}$$

The relative position of the neutral axis also effects the limiting value of extreme fibre strain. When pure axial stress is applied, the neutral axis is at infinity and the maximum value of strain at failure becomes ϵ'_c. When the neutral axis is inside a member section i.e. $z_m/z_n \geqq 1$, the extreme fibre strain is $\epsilon_{cu\theta}$. When the neutral axis lies between these two limits i.e. when $z_m/z_n \leqq 1$, then the final adopted value of extreme fibre strain denoted by ϵ_u is given by the simple linear relation shown in Fig. 2c, where,

$$\frac{\epsilon_u}{\epsilon'_c} = 1+\left\{\frac{\epsilon_{cu}}{\epsilon'_c}[1+(k_2-1)\sin 2\theta]-1\right\}\frac{z_m}{z_n}. \tag{4}$$

From the strain distribution at failure shown in Fig. 2a the concrete strain ϵ_c at any fibre z from the origin can be expressed in terms of the limiting value ϵ_u as:

$$\epsilon_c = \epsilon_u\left(1-\frac{z}{z_n}\right). \tag{5}$$

This value can be expressed in normalised form as,

$$\frac{\epsilon_c}{\epsilon'_c} = \frac{\epsilon_u}{\epsilon'_c}\left[1-\frac{b}{z_n}\left(\frac{x}{b}\sin\theta+\frac{y}{t}\cos\theta\cdot\frac{t}{b}\right)\right]. \tag{6}$$

Similarly the normalised value of steel strain becomes,

$$\frac{\epsilon_s}{\epsilon_{sy}} = \frac{\epsilon_u}{\epsilon'_c}\frac{\epsilon'_c}{\epsilon_{sy}}\left[1-\frac{b}{z_n}\left(\frac{x}{b}\sin\theta+\frac{y}{t}\cos\theta\cdot\frac{t}{b}\right)\right]. \tag{7}$$

Expressing the strains in array notation, the concrete strain ϵ_{cij} at the centroid of an element ΔA_{cij} can be found from,

$$\frac{\epsilon_{cij}}{\epsilon'_c} = \frac{\epsilon_u}{\epsilon'_c}\left[1-\frac{b}{z_n}\left(\frac{x_{cj}}{b}\sin\theta+\frac{y_{ci}}{t}\cos\theta\cdot\frac{t}{b}\right)\right]. \tag{6a}$$

Similarly the steel strain ϵ_{sij} at the centroid of an element ΔA_{sij} can be found from,

$$\frac{\epsilon_{sij}}{\epsilon_{sy}} = \frac{\epsilon_u}{\epsilon'_c}\frac{\epsilon'_c}{\epsilon_{sy}}\left[1-\frac{b}{z_n}\left(\frac{x_{sj}}{b}\sin\theta+\frac{y_{si}}{t}\cos\theta\cdot\frac{t}{b}\right)\right]. \tag{7a}$$

Equilibrium Conditions

For equilibrium, the forces acting on elemental areas when summed over the cross-section of a member and the moments about the $0x$ and $0y$ axes; must equal P_u, $P_u e_y$ and $P_u e_x$ respectively. In all relationships a term repre-

senting the small force acting on the elemental area displaced by the steel should be included. However in a previous paper [13] it has been shown that for rectangular sections having a maximum steel ratio with $q = 1.0$, the change in the computed axial capacity caused by neglecting this small force was about 1% consequently this refinement has been ignored in the following equations.

For equilibrium, the sum of small forces acting on the steel and concrete elemental areas can be equated to P_u as,

$$P_u = \sum_i^{n_{ct}} \sum_j^{n_{cb}} f_{cij} \Delta A_{cij} + \sum_i^{n_{st}} \sum_j^{n_{sb}} f_{sij} \Delta A_{sij}.$$

For the cases where regularly spaced grids are used to partition the concrete and steel areas, the elemental areas ΔA_{cij} and ΔA_{sij} are constant over a member cross section. Then using the following expressions,

$$R_{cij} = \frac{f_{cij}}{k_1 f'_c}, \qquad R_{sij} = \frac{f_{sij}}{f_{sy}}, \qquad \Delta A_{sij} = p \Delta A_{cij} \frac{n_c}{n_s}, \qquad q' = \frac{n_c}{n_s} \frac{p f_{sy}}{k_1 f'_c}$$

one may write,

$$P_u = k_1 f'_c \Delta A_c \{ \sum_i^{n_{ct}} \sum_j^{n_{cb}} R_{cij} + q' \sum_i^{n_{st}} \sum_j^{n_{sb}} R_{sij} \}. \tag{8}$$

For the particular case when the axial force P_0 is applied the strain and stresses in the concrete and steel are uniform all over the section. Collapse occurs when the strain first reaches ϵ'_c irrespective of the steel stress and for this condition the steel stress ratio R_{sij} attains a constant value R_{s0} where,

$$R_{s0} = \frac{f_s}{f_{sy}} = \frac{\epsilon'_c}{\epsilon_{sy}} \quad \text{provided} \quad \epsilon'_c \leqq \epsilon_{sy}.$$

When $\epsilon'_c / \epsilon_{sy} \geqq 1$ the steel yields and $R_{s0} = 1.0$.

The axial force P_0 can be found from the expression,

$$P_0 = k_1 f'_c n_c \Delta A_c + f_s n_s \Delta A_s = k_1 f'_c \Delta A_c \left\{ n_c + \frac{n_s R_{s0} f_{sy} p n_c}{k_1 f'_c n_s} \right\},$$

hence

$$\frac{P_u}{P_0} = \frac{\sum_i^{n_{ct}} \sum_j^{n_{cb}} R_{cij} + q' \sum_i^{n_{st}} \sum_j^{n_{sb}} R_{sij}}{n_c + n_s R_{s0} q'} \tag{9}$$

For equilibrium, the sum of moments of the elemental forces about the $0x$ axis can be written,

$$P_u e'_y = \sum_i^{n_{ct}} \sum_j^{n_{cb}} f_{cij} \Delta A_{cij} y_{ci} + \sum_i^{n_{st}} \sum_j^{n_{sb}} f_{sij} \Delta A_{sij} y_{si}$$

$$= k_1 f'_c \Delta A_c \{ \sum_i^{n_{ct}} \sum_j^{n_{cb}} R_{cij} y_{ci} + q' \sum_i^{n_{st}} \sum_j^{n_{sb}} R_{sij} y_{si} \}.$$

Dividing by $P_u t$ one obtains

$$\frac{e'_y}{t} = \frac{\sum_i^{n_{ct}} \sum_j^{n_{cb}} R_{cij} \frac{y_{ci}}{t} + q' \sum_i^{n_{st}} \sum_j^{n_{sb}} R_{sij} \frac{y_{si}}{t}}{\sum_i^{n_{ct}} \sum_j^{n_{cb}} R_{cij} + q' \sum_i^{n_{st}} \sum_j^{n_{sb}} R_{sij}}. \tag{10}$$

Similarly for equilibrium, the sum of moments of the elemental forces about the $0y$ axis may be expressed as,

$$\begin{aligned} P_u e'_x &= \sum_i^{n_{ct}} \sum_j^{n_{cb}} f_{cij} \Delta A_{cij} x_{cj} + \sum_i^{n_{st}} \sum_j^{n_{sb}} f_{sij} \Delta A_{sij} x_{sj} \\ &= k_1 f'_c \Delta A_c \{ \sum_i^{n_{ct}} \sum_j^{n_{cb}} R_{cij} x_{cj} + q' \sum_i^{n_{st}} \sum_j^{n_{sb}} R_{sij} x_{sj} \}. \end{aligned}$$

Dividing by $P_u b$ it follows that,

$$\frac{e'_x}{b} = \frac{\sum_i^{n_{ct}} \sum_j^{n_{cb}} R_{cij} \frac{x_{cj}}{b} + q' \sum_i^{n_{st}} \sum_j^{n_{sb}} R_{sij} \frac{x_{sj}}{b}}{\sum_i^{n_{ct}} \sum_j^{n_{cb}} R_{cij} + q' \sum_i^{n_{st}} \sum_j^{n_{sb}} R_{sij}}. \tag{11}$$

Eqs. (9), (10) and (11) can now be solved by first assuming particular values for the non-dimensional material parameters $\epsilon_{sy}/\epsilon'_c$, $\epsilon_{cu}/\epsilon'_c$, and k_2 and particular cross-section parameters, t/b, t'/t, t''/t, b'/b, b''/b and q.

For the cases where irregularly spaced grids are used to partition a cross-section, the elemental areas ΔA_{cij} and ΔA_{sij} are not constant over the member area. In this case the arrays C, X_{cj}, Y_{ci}, S, X_{sj} and Y_{si} can be used to represent the cross-section dimensions and Eqs. (9), (10) and (11) can be replaced by Eqs. (9a), (10a) and (11a) where,

$$q'' = \frac{A_c}{n_s} q,$$

$$\frac{P_u}{P_0} = \frac{\sum_i^{n_{ct}} \sum_j^{n_{cb}} R_{cij} C_{ij} + q'' \sum_i^{n_{st}} \sum_j^{n_{sb}} R_{sij} S_{ij}}{\sum_i^{n_{ct}} \sum_j^{n_{cb}} C_{ij} + q'' R_{s0} \sum_i^{n_{st}} \sum_j^{n_{sb}} S_{ij}}. \tag{9a}$$

$$\frac{e'_y}{t} = \frac{\sum_i^{n_{ct}} \sum_j^{n_{cb}} R_{cij} C_{ij} \frac{Y_{ci}}{t} + q'' \sum_i^{n_{st}} \sum_j^{n_{sb}} R_{sij} S_{ij} \frac{Y_{si}}{t}}{\sum_i^{n_{ct}} \sum_j^{n_{cb}} R_{cij} C_{ij} + q'' \sum_i^{n_{st}} \sum_j^{n_{sb}} R_{sij} S_{ij}}, \tag{10a}$$

$$\frac{e'_x}{b} = \frac{\sum_i^{n_{ct}} \sum_j^{n_{cb}} R_{cij} C_{ij} \frac{X_{cj}}{b} + q'' \sum_i^{n_{st}} \sum_j^{n_{sb}} R_{sij} S_{ij} \frac{X_{sj}}{b}}{\sum_i^{n_{ct}} \sum_j^{n_{cb}} R_{cij} C_{ij} + q'' \sum_i^{n_{st}} \sum_j^{n_{sb}} R_{sij} S_{ij}}. \tag{11a}$$

It should be noted that in the above Eqs. (9a), (10a) and (11a) the elements C_{ij} are the actual concrete elemental areas whereas the elements S_{ij} are represented by numbers. When the elements S_{ij} are the actual steel elemental areas divided by p then q'' should be replaced by q in the Eqs. (9a), (10a) and (11a).

The eccentricities of loading measured from the plastic centroid are,

$$e_x = 0.5\,b - e'_x$$

and

$$e_y = 0.5\,t - e'_y,$$

and the resultant eccentricity is,

$$e_r = \sqrt{e_x^2 + e_y^2}$$

or in non-dimensional form becomes,

$$\frac{e_r}{b} = \sqrt{\left(0.5 - \frac{e'_x}{b}\right)^2 + \left(\frac{t}{b}\right)^2 \left(0.5 - \frac{e'_y}{t}\right)^2}. \tag{12}$$

The direction of load measured from the $0x$ axis is defined by the angle ψ where,

$$\tan\psi = \frac{e_y}{e_x}$$

or

$$\psi = \tan^{-1}\left\{\frac{t}{b}\left(\frac{0.5 - \frac{e'_y}{t}}{0.5 - \frac{e'_x}{b}}\right)\right\}. \tag{13}$$

The equations derived in this section have been incorporated in a general computer program, written in Fortran IV language. The three values P_u/P_0, e_x/b and e_y/t can be determined from any chosen position and inclination of the neutral axis and a three dimensional failure surface plotted, using these values as the co-ordinate axes. Alternatively the values of P_u/P_0, ψ and e_r/b can be evaluated, from which two dimensional graphs containing failure curves can be drawn. The program has been used to study factors affecting the ultimate strength of concrete members. Often large changes in variables have little effect on the ultimate strength and approximations can be introduced, which while not unduly affecting the collapse load, lead to a great reduction in the number of charts required for a wide range of design problems.

Ultimate Strength Design

Design Charts

Owing to the large number of variables involved the theory has been presented in non-dimensional form to minimise the number of design charts required. The material properties have been expressed as ratios $\epsilon_{cu}/\epsilon'_c$, $\epsilon_{sy}/\epsilon'_c$

and as non-dimensional parameters k_1 and k_2 and in this paper, the values adopted for $\epsilon_{cu}/\epsilon'_c$, $\epsilon_{sy}/\epsilon'_c$ and k_2 are 1.1, 0.5 and 1.6 respectively. The value k_1 can be selected at will by the designer.

The variables relating to cross-section dimensions are the overall width b, hole width b'', overall depth t, total hole depth t'' and distances between side steel b' and top and bottom steel distance t'. By assuming the steel is placed along the mid-wall position and the wall thickness is small compared with the overall dimensions, the variables b, b'' and t, t'' can be replaced by b' and t' respectively, thus greatly reducing the number of variables. The design charts included in this paper only relate to the t'/b' ratio.

Two typical bridge pier sections were considered, one of rectangular hollow section and another of triple box section. The concrete cross-sections were partitioned into elemental areas by means of regularly spaced grids having n_{cb} columns and n_{ct} rows. The hollow rectangular section was partitioned by a 10×10 grid hence $n_{cb} = n_{ct} = 10$ and the triple box section partitioned by a 10×30 grid where $n_{cb} = 10$ and $n_{ct} = 30$. These grids minimised computational time while maintaining suitable accuracy and exactly subdivided the selected areas. The steel reinforcement for both cross-sections was simply partitioned by regularly spaced grids having n_{sb} columns and n_{st} rows where $n_{sb} = n_{st} = 10$. Although the axial capacity of sections subdivided by irregularly spaced grids were computed, they were only used for comparison of results obtained using regularly spaced grids and the data has not been included in the paper.

When compression and biaxial bending are applied to a multi-cell rectangular section the determination of the neutral axis position and direction is a rather tedious process. This difficulty is overcome by the reverse procedure of selecting the neutral axis position parameter z_n/b and direction angle θ and calculating the force P_u applied at eccentricities e_x and e_y, necessary to cause this particular selected position and direction of the neutral axis. By incrementing θ from 0° to 90° in 10° increments and at the same time varying z_n/b from 0.1 to 10.0 in 0.1 increments, the limiting value of extreme fibre strain ϵ_u can be found and from it the strains and stresses at the centroids of each concrete and steel element. The forces acting on elemental areas are then summed over the cross-section of the member and the moments about the $0x$ and $0y$ axes evaluated to find P_u/P_0, ψ and e_r/b. These calculations are required for particular values of steel ratio, so q was varied from 0 to 1.0 in 0.1 increments to provide sufficient data for the production of design charts.

Although these data are sufficient to produce three dimensional q constant surfaces, its accurate graphical representation is most difficult as seen from Fig. 6. This plotting difficulty can be overcome by finding the intersection lines between constant ψ vertical planes, which contain the P_u/P_0 axis and the constant q failure surfaces. These intersection lines can then be plotted on two dimension graphs for particular values of ψ. Obviously when a rectangular section is subjected to uniaxial bending about the $0x$ axis $\theta = 0°$ and $\psi = 90°$

and similarly for uniaxial bending about the $0y$ axis $\theta = 90°$ and $\psi = 0°$. For all other cases of biaxial bending, although integer values of θ are given, the computed ψ values are in general not whole numbers consequently a simple graphical interpolating procedure was adopted to obtain points for plotting the q constant lines required for integer values of ψ. In this paper two dimensional graphs are included for several cross-sections with $\psi = 0°$, 30°, 60° and 90° in Figs. 11a to 14c.

Effect of Variables on Strength

For simplicity of presentation, the effect of variables on the ultimate strength of a hollow square section having equal quantities of steel uniformly distributed around the mid-wall position will be examined. The dimension ratios of this section are $t/b = 1.0$, $t'/t = b'/b = 0.9$, $t''/t = b''/b = 0.8$ and both values of $q = 0$ and 1.0 will be compared for values of $\psi = 0°$, 45° and 90°.

Effect of Grid Size

The graphs presented in this paper for hollow square sections are based on a grid size where $n_{cb} = n_{ct} = n_{sb} = n_{st} = 10$. Another computer run was made using $n_{cb} = n_{ct} = 30$ and the comparison of varying n_{cb} and n_{ct} by 200% is shown in Fig. 7 resulting in a maximum variation of about 5% in the non-dimensionalised column capacity P_u/P_0. Obviously increasing the fineness of the concrete partitioning beyond a 10×10 grid has little effect on P_u/P_0 consequently this size was adopted for partitioning hollow rectangular sections.

In bridge piers it is usual to have equal quantities of steel adjacent to the four wall faces in hollow rectangular sections hence $n_{sb} = n_{st}$. Since many reinforcing bars are often used, these quantities of steel can be assumed uniformly distributed along their respective faces and in this paper $n_{sb} = n_{st} = 10$ has been adopted for computation of data for all pier sections examined. For comparison purposes additional data was computed with $n_{sb} = n_{st} = 30$ and plotted in Fig. 7. It can be seen that a 200% increase in steel grid fineness produced a maximum change of about 5% in the column strength ratio P_u/P_0 and 10×10 grids were considered sufficiently accurate for partitioning the steel area.

Effect of Ratio $\epsilon_{cu}/\epsilon'_c$ and k_2

Although the values adopted for ϵ_{cu} and ϵ'_c were 0.0022 and 0.002, only the ratio $\epsilon_{cu}/\epsilon'_c = 1.1$ was used in the production of data for the charts presented in this paper. The value of $\epsilon_{cu}/\epsilon'_c$ was increased by 200% to 3.3 and the case of uniaxial bending, when k_2 has no effect on column strength, was examined. The data plotted in Fig. 8a shows a maximum change in P_u/P_0 of about 10% indicating that the ratio $\epsilon_{cu}/\epsilon'_c$ has little effect on the strength capacity.

The parameter k_2 has its greatest effect on column strength when $\psi = 45°$ therefore a symmetrically reinforced hollow square section subjected to

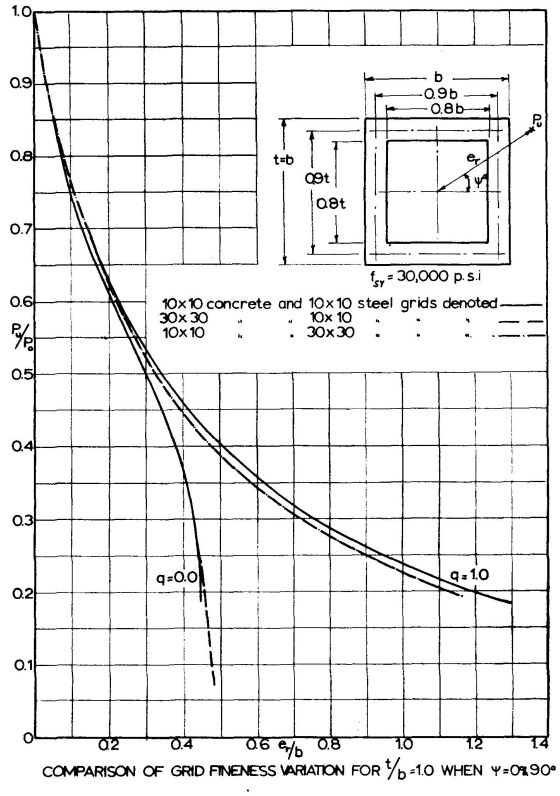

Fig. 7.

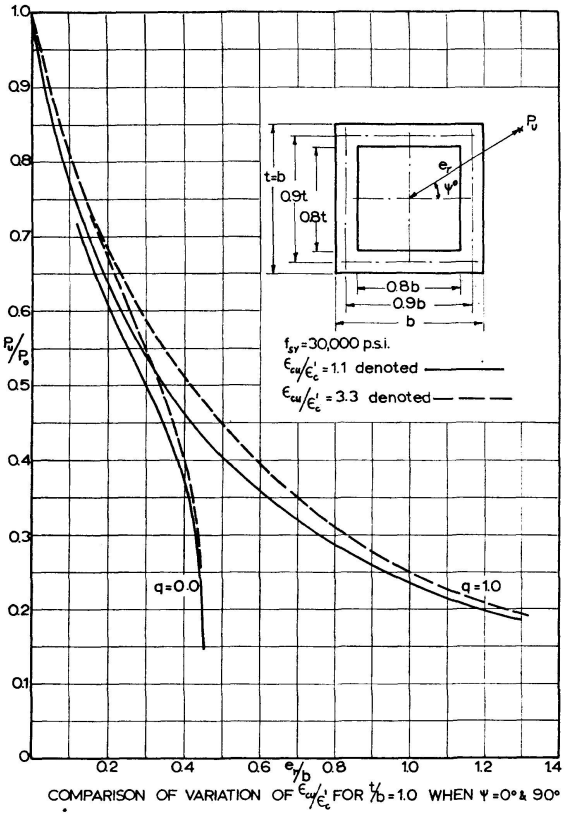

Fig. 8a.

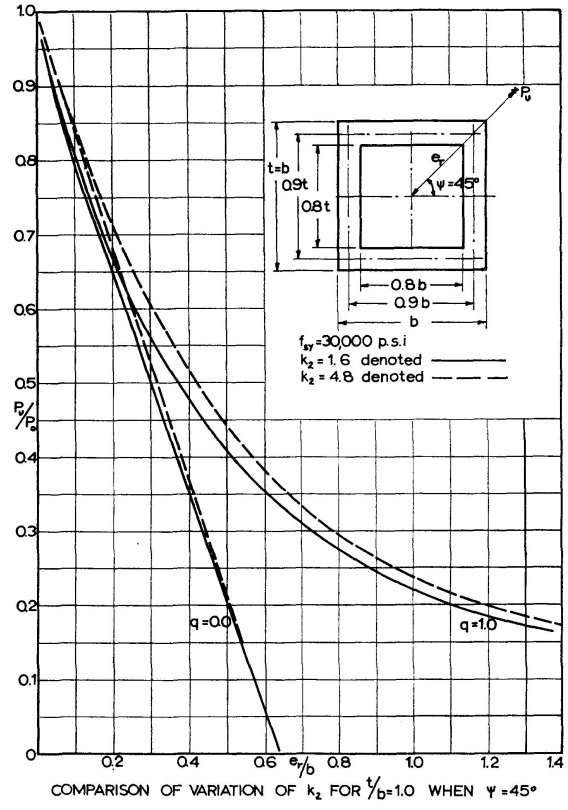

Fig. 8b.

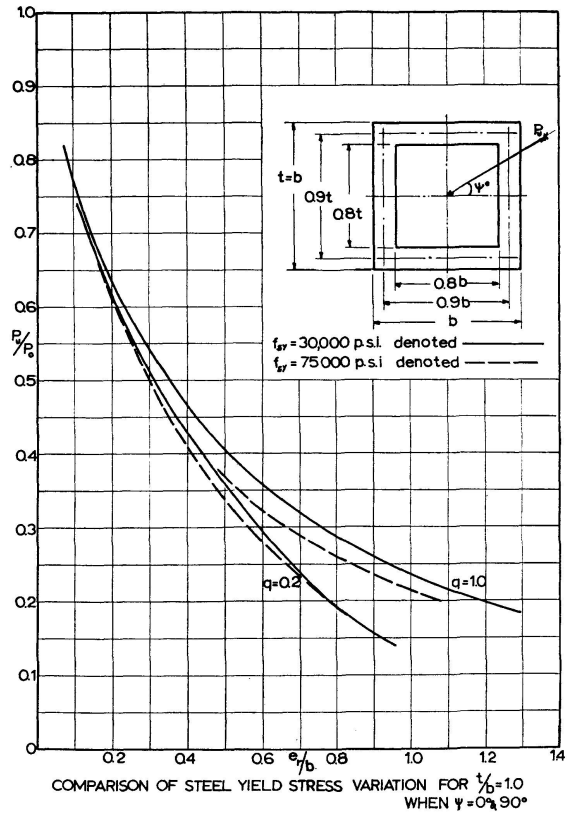

Fig. 9.

bending about a diagonal was examined. The value of k_2 was increased by 200% from its value of 1.6 adopted in this paper to 4.8 and the data plotted in Fig. 8b for comparison purposes. This variation of k_2 changed P_u/P_0 by about 9% hence a change of the parameter k_2 apparently has small effect on column strength.

Effect of Ratio $\epsilon_{sy}/\epsilon'_c$

The yield stress f_{sy} of commercially available reinforcing steels varies from about 30,000 to 75,000 psi and when the steel modulus of elasticity is 30×10^6 psi, the yield strain ϵ_{sy} changes from 0.001 to 0.0025 respectively. To determine the effect on column strength when ϵ_{sy} was varied from 0.001 to 0.0025 a symmetrical square column was examined. The effect on ultimate strength of changing $\epsilon_{sy}/\epsilon'_c$ by 150% can be seen in Fig. 9 where the results of both steels having steel ratios of $q=0.2$ and 1.0 are plotted for comparison purposes. For the high steel ratio of $q=1.0$, the maximum variation of the strength ratio P_u/P_0 was about 9% and for $q=0.2$, only 5% variation occurred in P_u/P_0. Obviously $q=0$ indicates that no reinforcement is used and variation of ϵ_{sy} cannot effect the column strength ratio. Bridge piers often contain low steel proportions where q is generally less than 0.2, and variation in the strain ratio $\epsilon_{sy}/\epsilon'_c$ has neglegible effect on P_u/P_0 for most cases. This means that the charts included in this paper for mild steel can be used without appreciable error for the ultimate strength design of columns when any strength commercially available reinforcing bars are contemplated. It should be noted that although the strength ratio P_u/P_0 is not greatly affected by change in the strain ratio $\epsilon_{sy}/\epsilon'_c$, the steel yield strain ϵ_{sy} or its related stress f_{sy} directly effects the value of P_0 since $P_0 = k_1 f'_c A_c + f_{sy} A_s$ consequently the ultimate strength P_u is directly related to the steel yield stress f_{sy}.

Effect of Wall Thickness

If the wall thickness is small compared with the cross-section dimensions and if the steel is located along the mid-wall position then it was believed possible to replace b and b'' with b' and t and t'' with t' without undue loss of accuracy of the computed axial capacity. To examine the possibility of making b, b'', t and t'' redundant and so greatly reducing the number of required design graphs, both a hollow square and a thin-wall triple box section were examined where the side wall thickness was either zero or $0.1\,b$ and the transverse wall thickness was either zero or $0.1\,t$.

The data for a square section column are plotted on Fig. 10a for values of $q=0$ and 1.0, where it can be seen that for a steel ratio $q=1$, the maximum variation of the ratio P_u/P_0 is about 12%. When no steel is used or $q=0$ and for an e_r/b value 0.4 i.e. when tensile cracking is about to commence in the column section, the variation of P_u/P_0 is about 24%. However non-reinforced concrete columns subjected to possible tensile stress should be rare, conse-

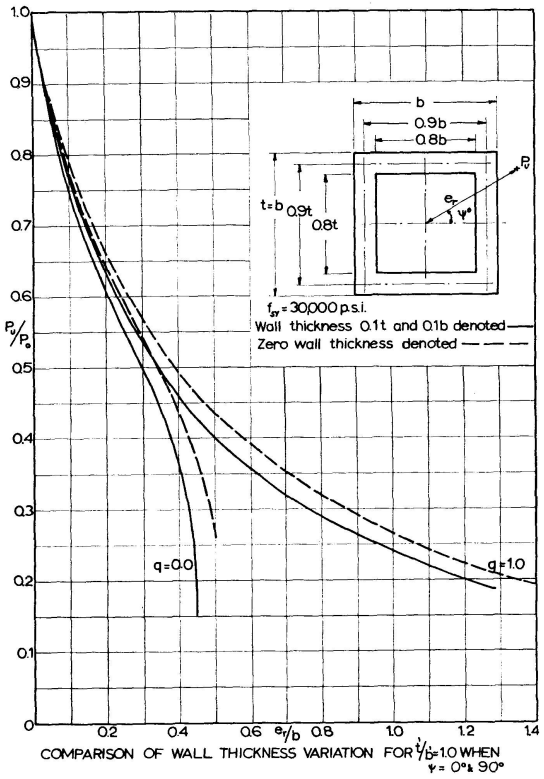

Fig. 10a.

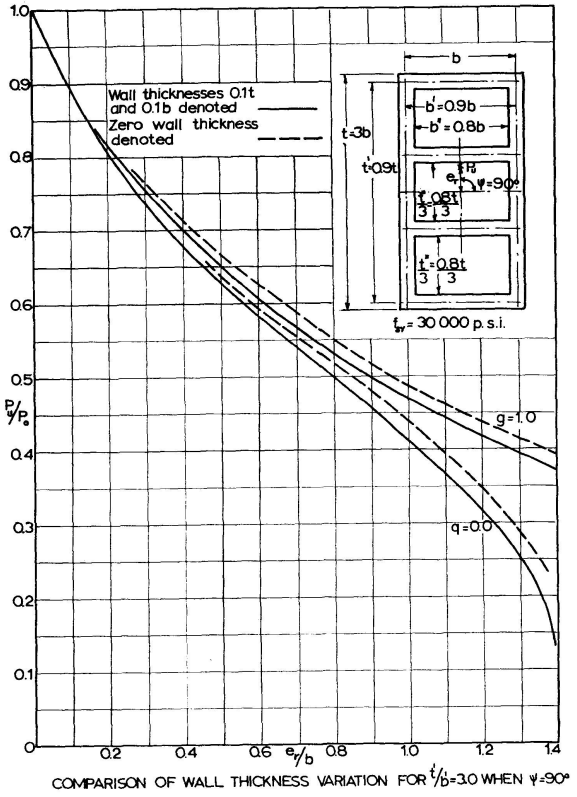

Fig. 10b.

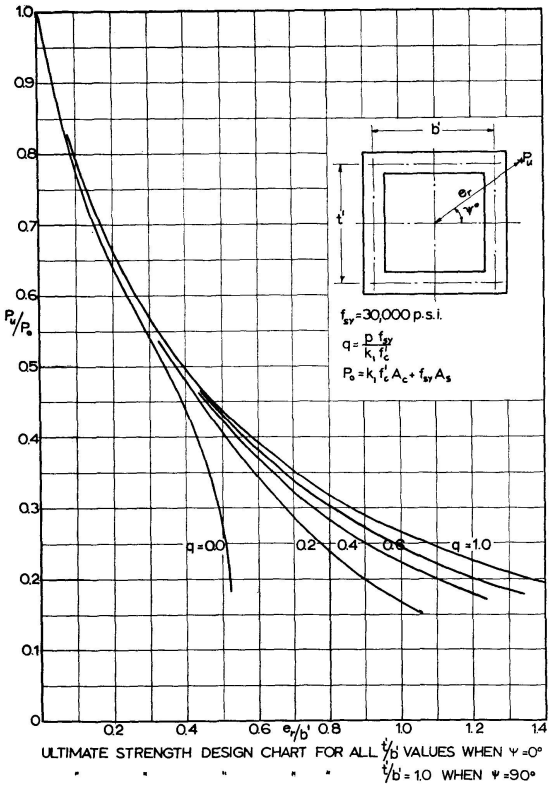

Fig. 11a.

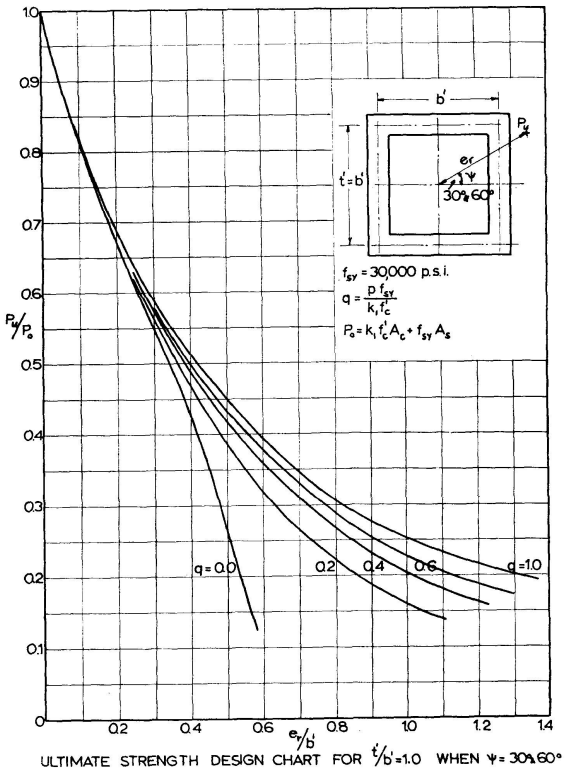

Fig. 11b.

quently the assumption of zero wall thickness will in most cases give reasonable estimation of the strength capacity ratio P_u/P_0.

The results for the thin-wall triple box section examined are included on Fig. 10b where it can be seen that for $q=0$ and 1.0 the maximum variation in the ratio P_u/P_0 was by about 15% and 4% respectively as the wall thickness changed from $0.1t$ and $0.1b$ to zero. The author believes the accuracy of predicting the ultimate capacity ratio P_u/P_0 of thin walled sections is therefore sufficient when the walls are assumed to have zero thickness.

It should be noted, however, that although the walls are assumed to have zero thickness for the computation of the ratio P_u/P_0, the wall thickness directly effects the value of P_0 which equals $k_1 f'_c A_c + f_{sy} A_s$ since the area of concrete A_c is related to the wall thickness. Obviously the ultimate strength of a column P_u is directly related to the wall thickness.

Design Examples

Example 1

Design a hollow rectangular symmetrically reinforced bridge pier to support a longitudinal force $P_u = 12{,}000$ kips at eccentricities of $e_x = 10\sqrt{3}$ in. and $e_y = 10$ in. when the effective concrete strength $k_1 f'_c = 3{,}000$ psi and mild steel with yield stress $f_{sy} = 30{,}000$ psi are used.

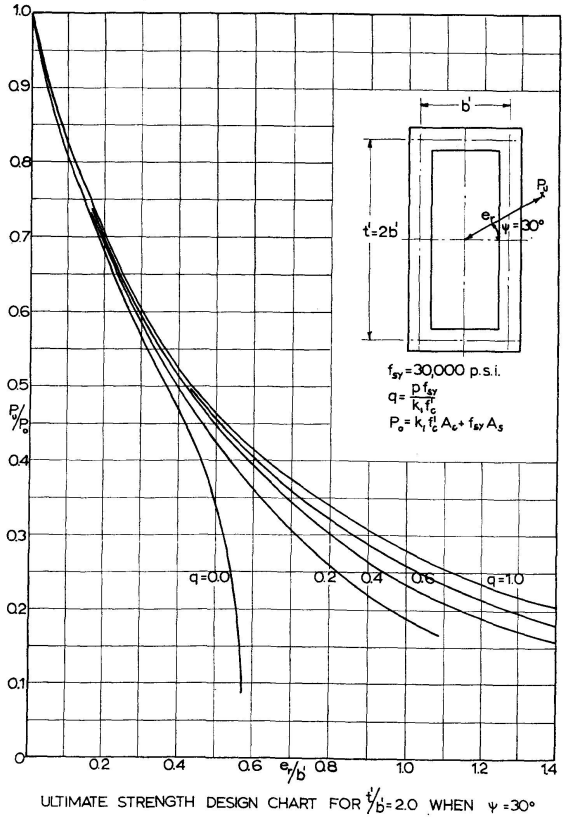

ULTIMATE STRENGTH DESIGN CHART FOR $t'/b' = 2.0$ WHEN $\psi = 30°$

Fig. 12a.

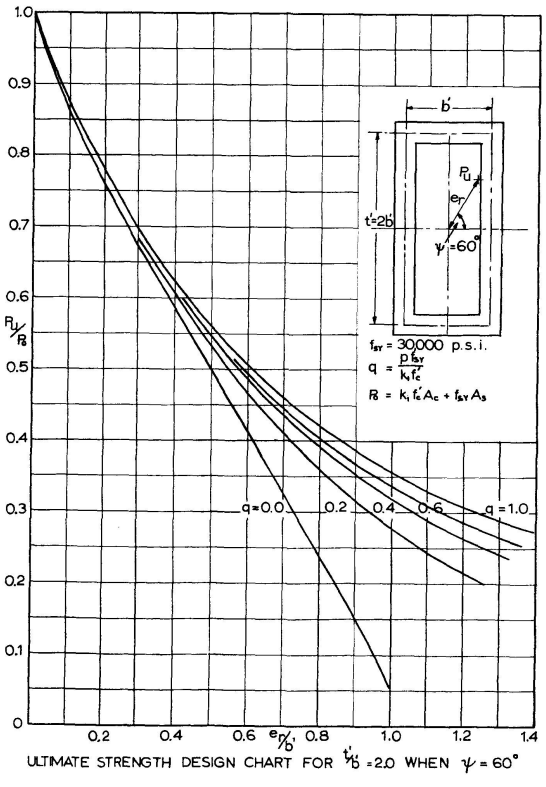

ULTIMATE STRENGTH DESIGN CHART FOR $t'/b' = 2.0$ WHEN $\psi = 60°$

Fig. 12b.

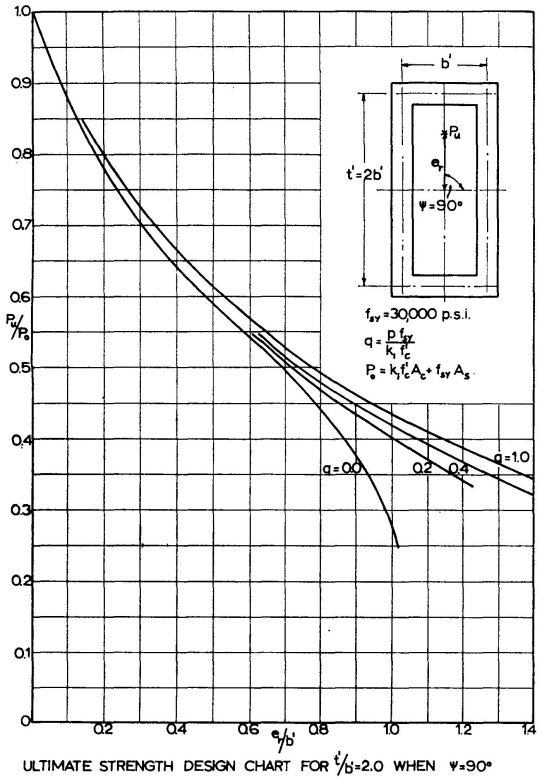

ULTIMATE STRENGTH DESIGN CHART FOR t'/b=2.0 WHEN ψ=90°

Fig. 12c.

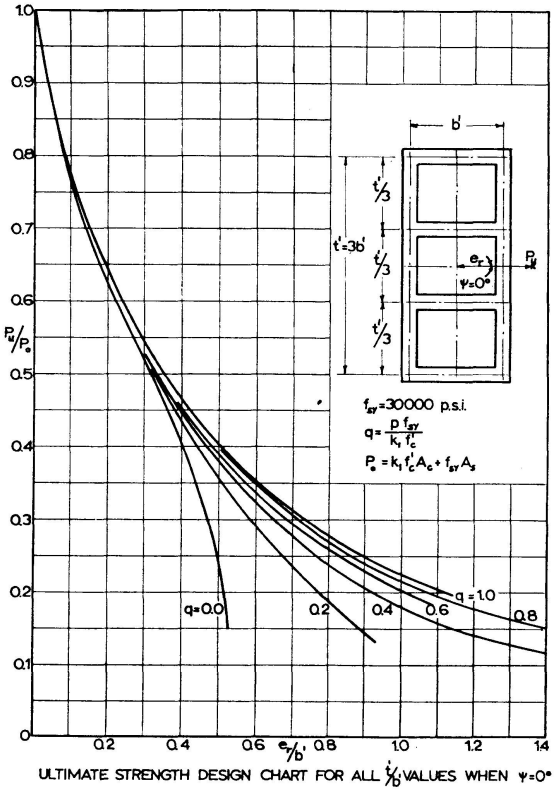

ULTIMATE STRENGTH DESIGN CHART FOR ALL t'/b VALUES WHEN ψ=0°

Fig. 13a.

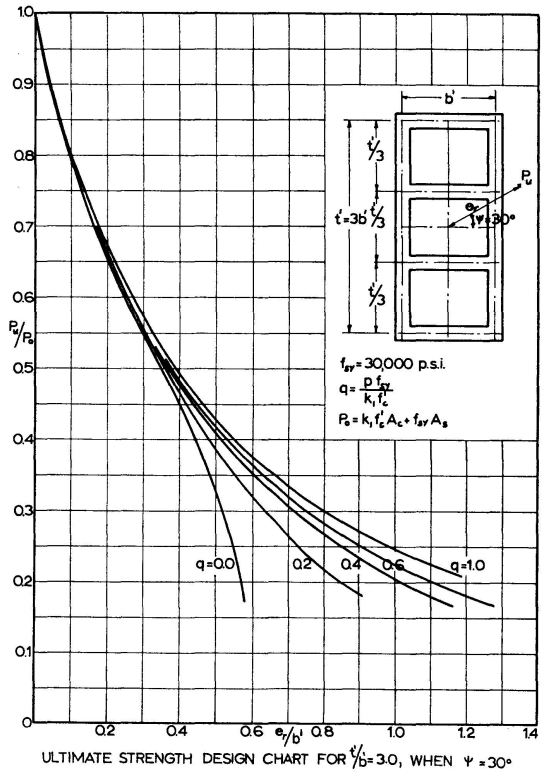

ULTIMATE STRENGTH DESIGN CHART FOR t'/b=3.0, WHEN ψ=30°

Fig. 13b.

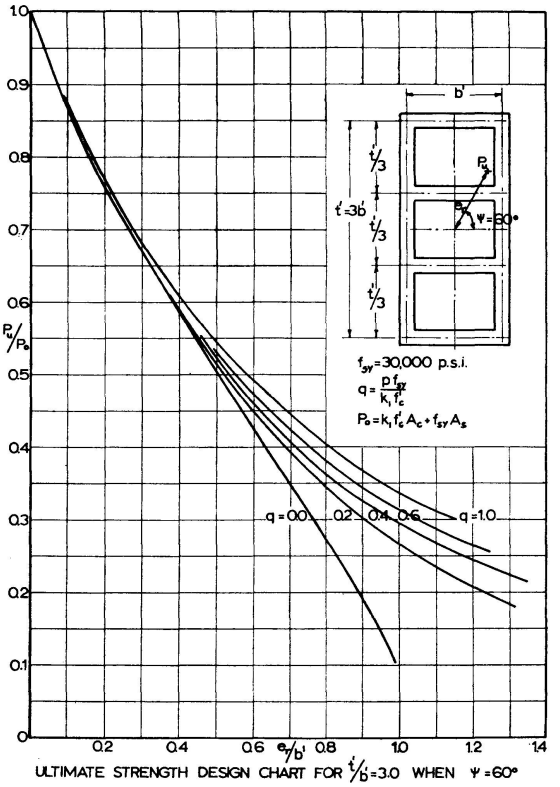

ULTIMATE STRENGTH DESIGN CHART FOR t'/b=3.0 WHEN ψ=60°

Fig. 13c.

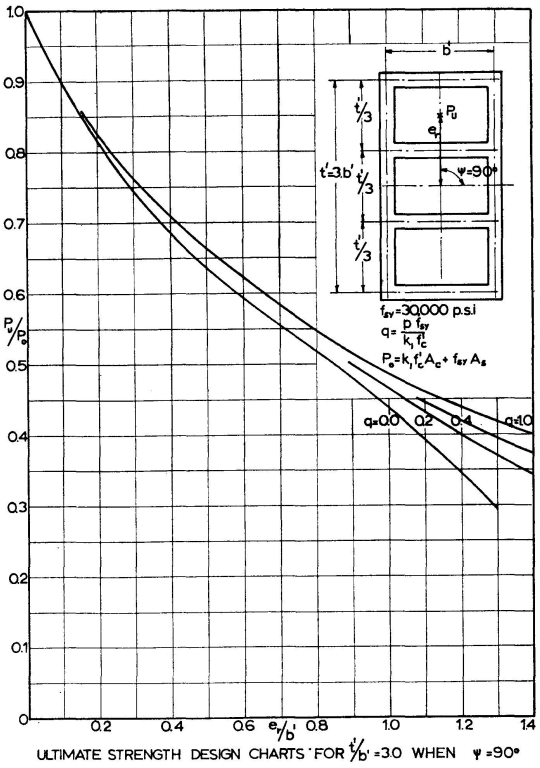

Fig. 13d.

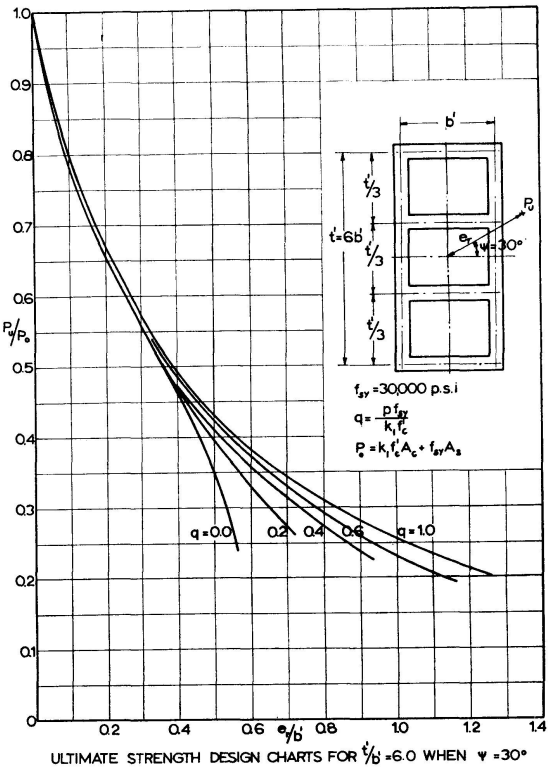

Fig. 14a.

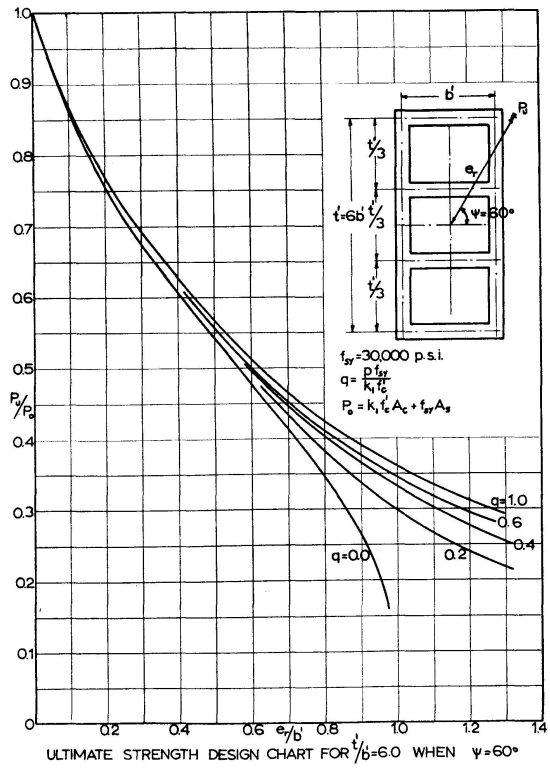

Fig. 14b.

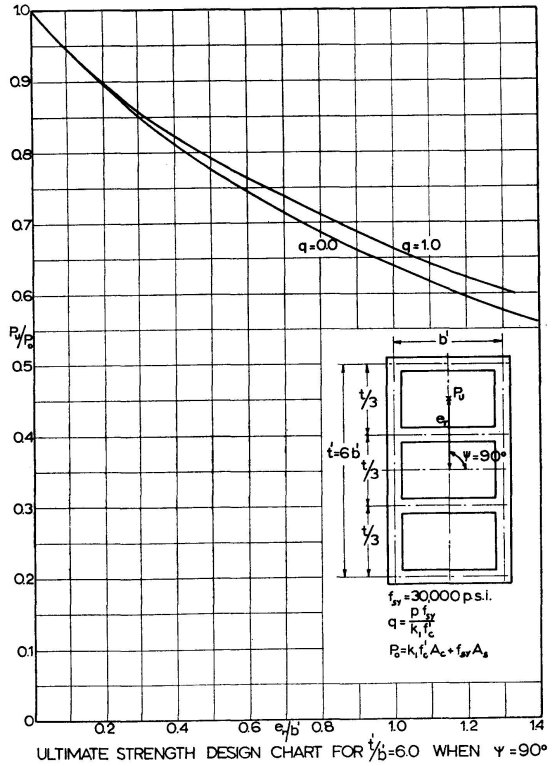

Fig. 14c.

Assuming an average concrete stress of 2,000 psi, a steel proportion of about 0.002, a wall thickness of 10″, a mid-wall position dimension ratio $t'/b' = 2$, then a pier having approximate dimensions 10 ft. × 20 ft. may suffice. When $b = 110$ in., $t = 210$ in., $b' = 100$ in., $t' = 200$ in., $b'' = 90$ in. and $t'' = 190$ in. then $A_c = 6000\,\text{in}^2$ and $A_s = 12\,\text{in}^2$. Using 2 layers of one gauge mesh at 6 in centres having $0.283\,\text{in}^2$ of steel per foot length of wall, then the total $A_s = 14.1\,\text{in}^2$. When placing one steel layer adjacent to the inner and outer faces of all walls so that the mean steel position is along the mid-wall line, then $t'/b' = 2$. Now $e_r = 20$ in., $\psi = 30°$, $e_r/b' = 0.2$ and $q = 0.02$, then from the related graph Fig. 12a, $P_u/P_0 = 0.68$.

Now $$P_0 = 3000 \times 6000 + 14.1 \times 30{,}000 = 18{,}420 \text{ kips},$$

$$\therefore\ P_u = 0.68 \times 18{,}420 \text{ kips} = 12{,}500 \approx 12{,}000 \text{ kips}.$$

Example 2

Design a multi-cell rectangular reinforced concrete bridge pier having two internal diaphrams to support a longitudinal force $P_u = 20{,}000$ kips placed at eccentricities of $e_x = 50$ in. and $e_y = 50\sqrt{3}$ in. when the effective concrete strength $k_1 f'_c$ and the steel yield stress f_{sy} are 3,000 and 30,000 psi respectively.

Assuming an average concrete stress of 1000 psi a steel proportion of about 0.002, a wall thickness of 10 in., a mid-wall dimension ratio $t'/b' = 3$, then try a pier of 10 ft. × 30 ft. mean dimensions. When $b = 130$ in., $t = 370$ in., $b' = 120$ in., $t' = 360$ in., $b'' = 110$ in., $t'' = 330$ in. then $A_c = 11{,}700\,\text{in}^2$ and $A_s = 23.4\,\text{in}^2$. Now 2 layers of 2 gauge mesh at 6 in. centres has $0.2392\,\text{in}^2$ of steel per foot run of wall, then the total $A_s = 23.9\,\text{in}^2$. Provided the mean steel position is placed along the mid wall line then $t'/b' = 3.0$. As $e_r = 100$ in., $\psi = 60°$, $e_r/b' = 0.833$ and $q = 0.02$, then from the related graph Fig. 13c, $P_u/P_0 = 0.26$.

Now $$P_0 = 11700 \times 3{,}000 + 23.9 \times 30{,}000 = 35{,}815 \text{ kips},$$

$$\therefore\ P_u = 0.26 \times 35{,}815 = 9300 \approx 9{,}000 \text{ kips}.$$

Hence the selected sections in both examples are satisfactory.

Conclusions

The method presented for the ultimate strength design of sections subjected to compression and biaxial bending is arranged for computer solution. The method is based on partitioning a member cross-section into many discrete elemental areas to simplify the complications induced by various non-linear stress distributions at failure acting over any non-symmetrical area. The tedious integrations with many discontinuities and awkward limits are thus eliminated by the partitioning process and the use of a computer to sum the actions.

Although any possible non-linear stress distribution can be accomodated, the method is also useful for elastic stress design of the most complicated cross-sections. Since ultimate strength methods are not generally permitted by the design codes, the method presented has immediate use for working stress design of multi-cell bridge piers subjected to tensile stresses over part of the cross-section. A simpler program for the generation of data has been run for the publication of working stress design curves at a later date.

The criterion for failure in this analysis is the limiting value of extreme fibre strain and once concrete reaches this value failure is assumed imminent. Other factors affecting material properties such as insufficient compaction of concrete in the finished structure, poor workmanship, lateral buckling of the longitudinal reinforcement, etc., have been ignored. Until such time as this theory is supported by test results of reasonably sized hollow test specimens it would be prudent to either increase the load factors or to reduce the computed ultimate capacity by means of a suitable strength reduction factor [6].

Acknowledgements

This work was carried out in the Department of Structures at the University of New South Wales and is part of a study undertaken by Dr. R. F. Warner and the author. Mr. M. Taylor of the Structures Laboratory assisted both with the preparation of programmes and the production of the design graphs. The computer programme was executed on the IBM system 360-50 computer in the School of Electical Engineering of this University.

References

1. Bresler, B.: Design criteria for reinforced columns under axial load and biaxial bending. J. A. C. I., Vol. 32 No. 5, Nov. 1960, pp. 481—490 (Proc. A. C. I. Vol. 57).
2. Meek, J. L.: Ultimate strength of columns with biaxial eccentric loads. J. A. C. I. No. 8, Aug. 1963, pp. 1053—1064 (Proc. A. C. I. Vol. 60).
3. Pannell, F. N.: Design charts for members subjected to biaxial bending and thrust. Concrete Publications Ltd., 1966, 51 p.
4. Weber, D. C.: Ultimate strength design charts for columns with biaxial bending. J. A. C. I. No. 11, Nov. 1966, pp. 1205—1230 (Proc. A. C. I. Vol. 63).
5. Seddon, A. E.: The strength of concrete walls under axial and eccentric loads. Symposium on the strength of concrete structures, London, May 1956, pp. 445—486.
6. American Concrete Institute: Building code requirements for reinforced concrete. A. C. I. 318—363, 1965, 144 p.
7. Standards Association of Australia. S. A. A code for concrete in buildings. CA 2—1963, 137 p.
8. American Concrete Institute and Cement and Concrete Association: Recommendations for an international code of practice for reinforced concrete. A. C. I. 1965, 156 p.
9. Rüsch, H.: Researches towards a general flexural theory for structural concrete. J. A. C. I. Vol. 32, No. 1, July 1960, pp. 1—28 (Proc. A. C. I. Vol. 57).

10. WARNER, R. F. and BRETTLE, H. J.: Ultimate strength design of thin-wall circular bridge piers. Publications of the International Association for Bridge and Structural Engineering, Vol. 27, 1967, Zurich.
11. BRETTLE, H. J. and WARNER, R. F.: Theory for the ultimate strength design of hollow circular concrete sections. Symposium on concrete structures, Institution of Engineers Aust., Sydney, 1967, pp. 109—115.
12. WARNER, R. F. and BRETTLE, H. J.: Strength of reinforced concrete in biaxial bending and compression. University of New South Wales, Dept. of Civ. Eng. UNICIV Report No. R-24, Nov. 1967.
13. BRETTLE, H. J. and WARNER, R. F.: Ultimate strength design of rectangular reinforced concrete sections in compression and biaxial bending. Civ. Engg. Trans. I. E. Aust., Vol. CE 10, No. 1, April 1968.

Summary

Theory is presented for the ultimate strength design of thin-wall, multicell, rectangular reinforced concrete bridge piers when subjected to compression and biaxial bending. The analysis is based on sub-dividing a pier cross-section into many discrete parts and summing the forces acting on these elemental areas by means of a computer. Data were generated for the preparation of charts for the ultimate strength design of both hollow rectangular and triple box sections. Design charts for two different width to depth ratios are included for the simplification of the design procedure.

Résumé

On présente ici une théorie pour le calcul à la résistance limite de piles de ponts de section rectangulaire, multicellulaire, à parois minces en béton armé, soumises à la compression et à la flexion biaxiale. Le calcul, fait à l'aide d'un ordinateur, consiste en une sous-division de la section de la pile en nombreuses parties distinctes et en une addition des forces agissant sur ces éléments de surface. Des données ont été travaillées pour la préparation de graphiques pour le calcul de la résistance limite de sections creuses et de sections tricellulaires. On a inclus pour une simplification du dimensionnement des graphiques avec deux valeurs différentes du rapport largeur sur profandeur.

Zusammenfassung

Für den Fall «Druck mit zweiaxialer Biegung» wird das Traglastverfahren für dünnwandige, mehrzellige sowie rechteckige Eisenbeton-Brückenpfeiler angegeben. Das Verfahren unterteilt den Brückenquerschnitt in viele endliche Teile und summiert deren Kräfte mittels des Elektronenrechners. Ergebnisse wurden in Vorbereitung von Kurven für den hohlen und dreikastigen Querschnitt entwickelt. Zur Vereinfachung der Bemessung sind Kurven für zwei verschiedene Breiten- und Tiefenverhältnisse angegeben.